



## How close to the O(6) symmetry is the nucleus $^{124}\text{Xe}$ ?

G. Rainovski<sup>a,\*</sup>, N. Pietralla<sup>b</sup>, T. Ahn<sup>d,b,c</sup>, L. Coquard<sup>b</sup>, C.J. Lister<sup>e</sup>, R.V.F. Janssens<sup>e</sup>, M.P. Carpenter<sup>e</sup>, S. Zhu<sup>e</sup>, L. Bettermann<sup>f</sup>, J. Jolie<sup>f</sup>, W. Rother<sup>f</sup>, R.V. Jolos<sup>g</sup>, V. Werner<sup>d</sup>

<sup>a</sup> Faculty of Physics, St. Kliment Ohridski University of Sofia, 1164 Sofia, Bulgaria

<sup>b</sup> Institut für Kernphysik, Technische Universität Darmstadt, D-64289 Darmstadt, Germany

<sup>c</sup> Department of Physics and Astronomy, SUNY at Stony Brook, Stony Brook, NY 11794-3800, USA

<sup>d</sup> Wright Nuclear Structure Laboratory, Yale University, New Haven, CT 06520-8120, USA

<sup>e</sup> Physics Division, Argonne National Laboratory, 9700 South Cass Avenue, Argonne, IL 60439, USA

<sup>f</sup> Institut für Kernphysik, Universität zu Köln, D-50937 Köln, Germany

<sup>g</sup> Joint Institute for Nuclear Research, RU-141980 Dubna, Russia

### ARTICLE INFO

#### Article history:

Received 5 August 2009

Received in revised form 1 December 2009

Accepted 6 December 2009

Available online 11 December 2009

Editor: V. Metag

#### PACS:

21.10.Re

23.20.Js

25.70.De

27.60.+j

#### Keywords:

Coulomb excitation reactions

Lifetime measurements

$B(E2)$  transition strengths

Collective models – IBM-1

### ABSTRACT

Excited states in  $^{124}\text{Xe}$  have been studied via the  $^{12}\text{C}(^{124}\text{Xe}, ^{124}\text{Xe}^*)$  Coulomb excitation reaction. Their population cross-sections relative to the  $2_1^+$  state have been determined from the  $\gamma$ -ray yields observed with Gammasphere. More than twenty absolute  $E2$  strengths for seven off-yrast, low-spin states of  $^{124}\text{Xe}$  have been deduced for the first time. The absolute  $B(E2)$  values indicate pronounced O(5) symmetry, even for the off-yrast states with high O(5) quantum number  $\tau$ , while the O(6) symmetry is substantially broken.

© 2009 Elsevier B.V. All rights reserved.

Symmetries offer powerful quantitative concepts in many fields of physics ranging from the formulation of the fundamental forces to the classification of many-body systems. In quantum mechanics the presence of a symmetry is related to conserved quantum numbers that can be established experimentally. Analogously, symmetry breaking is related to a situation in which the wave functions of the system contains many components with different quantum numbers. It is intriguing to study the questions when and how a symmetry dissolves on a quantitative basis. Nuclear collective excitations offer a unique quantum laboratory where this question can be studied experimentally. In nuclear physics, the three dynamical symmetries [1,2] of the Interacting Boson Model (IBM), U(5) [3], SU(3) [4], and O(6) [5] provide valuable benchmarks for the description of nuclear quadrupole collectivity at low and medium angular momenta. These three symmetries correspond to analytically

solvable cases of the geometrical Bohr Hamiltonian [6] – the harmonic vibrator, the quadrupole-deformed axial rotor, and the  $\gamma$ -unstable rotor [7]. Such idealized cases are never exactly observed in nature. Finding nuclides with behaviours close to expectations for specific dynamical symmetries is an intriguing task because such nuclei serve as benchmarks for the evolution of nuclear collectivity [8]. However, a quantitative answer to the question to what extent a certain dynamical symmetry is preserved or broken in such benchmark nuclei requires that one measure observables that are particularly sensitive to the symmetry under investigation. It is the purpose of this Letter to study the degree of O(6)-breaking in the case of  $^{124}\text{Xe}$ , a nucleus considered to be close to the O(6) dynamical symmetry [9].

The O(6) symmetry of the  $sd$ -IBM-1 is based on the chain  $U(6) \supset O(6) \supset O(5) \supset O(3)$  of nested sub-algebras with quantum numbers  $N$ ,  $\sigma$ ,  $\tau$ , and  $L$ , respectively [1,2]. The empirical evidence for the existence of nuclei at the O(6) dynamical limit of the IBM is based on energy level patterns, branching ratios and, more convincingly, on selection rules for  $E2$  transitions. Within the Con-

\* Corresponding author.

E-mail address: rig@phys.uni-sofia.bg (G. Rainovski).

sistent Q-Formalism (CQF) [10], they are such that  $E2$  transitions are allowed and collective only between states with  $\Delta\sigma = 0$  and  $\Delta\tau = \pm 1$  [2].<sup>1</sup> It is the  $\Delta\sigma = 0$  selection rule that is definitive of pure  $O(6)$  symmetry; the  $\Delta\tau = \pm 1$  selection rule is rather ubiquitous for all nuclei between  $U(5)$  and  $O(6)$  dynamical symmetries. A nucleus exhibiting an energy spectrum and decay patterns that can be classified in terms of  $\sigma, \tau, L$  quantum numbers and the respective selection rules is said to possess  $O(6)$  symmetry. Observation of  $O(6)$  symmetry in nuclei has first been reported in the case of  $^{196}\text{Pt}$  [12]. This claim was based on energy level patterns and  $E2$  decay branching ratios that closely follow the  $O(6)$  selection rules. It was, later on, supported by establishing a lower limit for the lifetime of the  $0_3^+$  state, the lowest state of the  $\sigma = N - 2$  representation [13]; the resulting upper limits for the absolute  $B(E2)$  values are small, in agreement with pure  $O(6)$  dynamical symmetry [13]. Another, even more extensive region of  $O(6)$ -candidate nuclei was found in the Xe–Ba–Ce region [9] around mass number  $A = 130$ . It has been shown that the low-spin structures of the nuclei  $^{128}\text{Xe}$  [14],  $^{126}\text{Xe}$  [15] and  $^{124}\text{Xe}$  [16] manifest  $O(6)$ -like arrangements of energy levels and  $E2$  branching ratios which reflect the selection rules for the  $\sigma = N$  states of  $O(6)$ .

On the other hand, the nuclei from the Pt and the Xe–Ba–Ce regions exhibit two systematic deviations from the exact  $O(6)$  symmetry, i.e., the smaller than expected energy staggering in the quasi- $\gamma$  bands and the  $\tau$ -compression effect [9]. These deviations can be accounted for by adding perturbative terms to the  $O(6)$  Hamiltonian [17]. These terms improve the description of the low-lying states with  $\sigma = N$  [16]. Quantifying the degree of symmetry preservation (or breaking), introduced by such realistic symmetry-perturbing terms is not an easy task because it, ideally, requires information on absolute  $E2$  transition rates, preferably between states with different  $O(6)$  quantum numbers. This crucial experimental information is either scarce [15,18,19] or often absent altogether. This is particularly true for transitions between off-yrast states, which supposedly belong to higher  $\tau \geq 3, 4$  and lower  $\sigma < N$  multiplets. Thus, due to the lack of data, a quantitative assessment of the goodness of the  $O(6)$  quantum number  $\sigma$  in the Xe–Ba region has not been performed to date. In this respect, the question of the extent in which the energies and the  $B(E2)$  branching ratios of levels with  $\sigma = N$  can serve as a unique signature for  $O(6)$ -like behaviour [20,21], especially for the off-yrast states, also remains open. To address these issues, we have measured absolute  $E2$  strengths between off-yrast, low-spin states of  $^{124}\text{Xe}$ .

A Coulomb excitation experiment was carried out at Argonne National Laboratory in inverse kinematics. The  $^{124}\text{Xe}$  beam, with intensity of  $\approx 1$  pnA ( $\sim 6 \times 10^9$  ions/s), was delivered by the ATLAS accelerator. It was incident on a  $1 \text{ mg/cm}^2$ -thick  $^{12}\text{C}$  target with an energy of 394 MeV. The deexcitation  $\gamma$  rays, following Coulomb excitation of the projectile, were detected with the Gammasphere array [22] which consisted of 98 HPGe detectors. Gammasphere was used in singles mode, resulting in an average counting rate of 8000 counts-per-second (cps), while the room background was producing about 600 cps. A total of  $5.1 \times 10^8$  events of  $\gamma$ -ray fold 1 or higher was collected in about 12 hours. The contribution of the room background was eliminated in the off-line sort by correlating the  $\gamma$  rays with the accelerator radio-frequency (RF) signal. The final spectrum, which is a difference between the “beam-on” (with respect to the RF) spectrum and the “beam-off” spectrum, scaled to eliminate the 1461-keV room back-

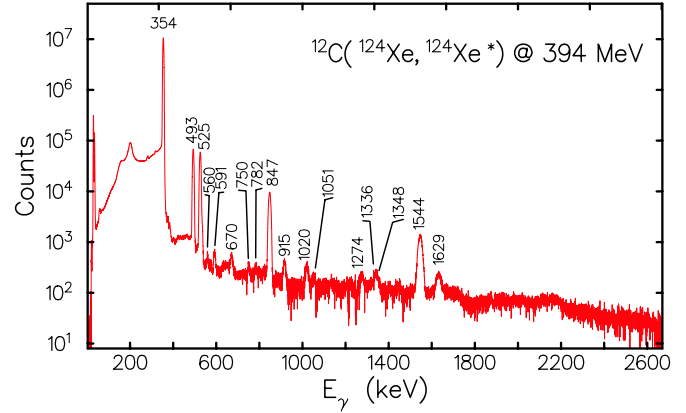


Fig. 1. (Color online.) Background-subtracted, Doppler-corrected  $\gamma$ -ray spectrum of  $^{124}\text{Xe}$  observed with Gammasphere after Coulomb excitation on a carbon target. The weak transitions in  $^{124}\text{Xe}$  are not indicated.

ground transition following the decay of  $^{40}\text{K}$ , is shown in Fig. 1. All  $\gamma$  rays in the spectrum originate from  $^{124}\text{Xe}$  nuclei recoiling with  $v/c \approx 6.3\%$ . Most of these  $\gamma$  rays have already been identified in  $^{124}\text{Xe}$  [16,23–25]. In addition, we have observed three new transitions with respective energies of 1051, 1413 and 1444 keV. About 4% of the data have  $\gamma$ -ray fold higher than 1. These events were sorted into a  $\gamma - \gamma$  coincidence matrix. The coincidence relationships and the energy balances suggest that the 1051-keV  $\gamma$  ray connects the  $3^-$  state at 1898 keV [25] to the  $2_2^+$  level at 847 keV. The latter two  $\gamma$  rays, at 1413 keV and the 1444 keV, depopulate a newly observed level at 2291 keV. The spectroscopic information is summarized in Table 1. The low-energy level scheme of positive-parity states of  $^{124}\text{Xe}$  is presented in Fig. 2(a). It agrees well with a general  $sd$ -IBM-1 calculation [16] fit to energy levels and  $E2$  branching ratios of  $^{124}\text{Xe}$  (cf. Table 1 and Tables 2 and 6 in Ref. [16]). The results from this calculation are presented in Fig. 2(b).

The relative  $\gamma$ -ray yields with respect to the  $2_1^+$  state measure the relative Coulomb excitation (CE) cross-sections. The contributions from electron conversion decays to the total depopulation of the  $^{124}\text{Xe}$  states are negligible, even for the decay of the  $0_2^+$  state at 1269 keV [24]. The  $\gamma$ -ray intensities of some transitions, unobserved in our experiment, were determined through the previously measured branching ratios in Ref. [16,24]. The experimental yields were fitted to the Winther–De Boer theory [26] with the multiple CE code CLX [27] by using the known value  $B(E2; 2_1^+ \rightarrow 0_1^+) = 0.2121(54)e^2b^2$  [19] and by taking into account the energy loss of the beam in the target. The signs of the  $E2$  matrix elements were chosen to be in agreement with the signs predicted by the IBM calculations [16]. Unknown quadrupole moments of excited states were varied between the extreme rotational limits, thereby introducing additional uncertainties in the deduced transition matrix elements of about 3%. Further details about the experiment and the analysis can be found in Ref. [28]. The resulting set of transition matrix elements provides the  $B(E2)$  transition strengths: those are presented in Table 1.

The energy levels of  $^{124}\text{Xe}$  with positive parity appear to form a pattern typical for  $O(6)$  symmetry (see Fig. 2). As noted in Ref. [16], for each eigenstate with  $O(6)$  quantum number  $\sigma = N$  a corresponding nuclear state can be found up to  $O(5)$  quantum number  $\tau = 5$  and angular momentum  $10\hbar$ , while the  $0_3^+$  and  $2_4^+$  states form a structure that resembles the bottom of the excited  $O(6)$  family with  $\sigma = N - 2$ . Therefore, it is reasonable to check whether the data on absolute  $E2$  strengths can be understood qualitatively in terms of  $O(6)$  ( $\Delta\sigma = 0$ ) and  $O(5)$  ( $\Delta\tau = \pm 1$ ) selection rules.

<sup>1</sup> The  $O(6)$  selection rules depend also on the choice of the  $E2$  operator. In its most general one-body form  $T(E2) = e(s^+ \tilde{d} + d^+ s + \chi_{E2} [d^+ \tilde{d}]^{(2)})$ , the  $E2$  operator also generates transitions between states with  $\Delta\tau = 0, \pm 2$  and  $\Delta\sigma = 0, \pm 2$  [11].

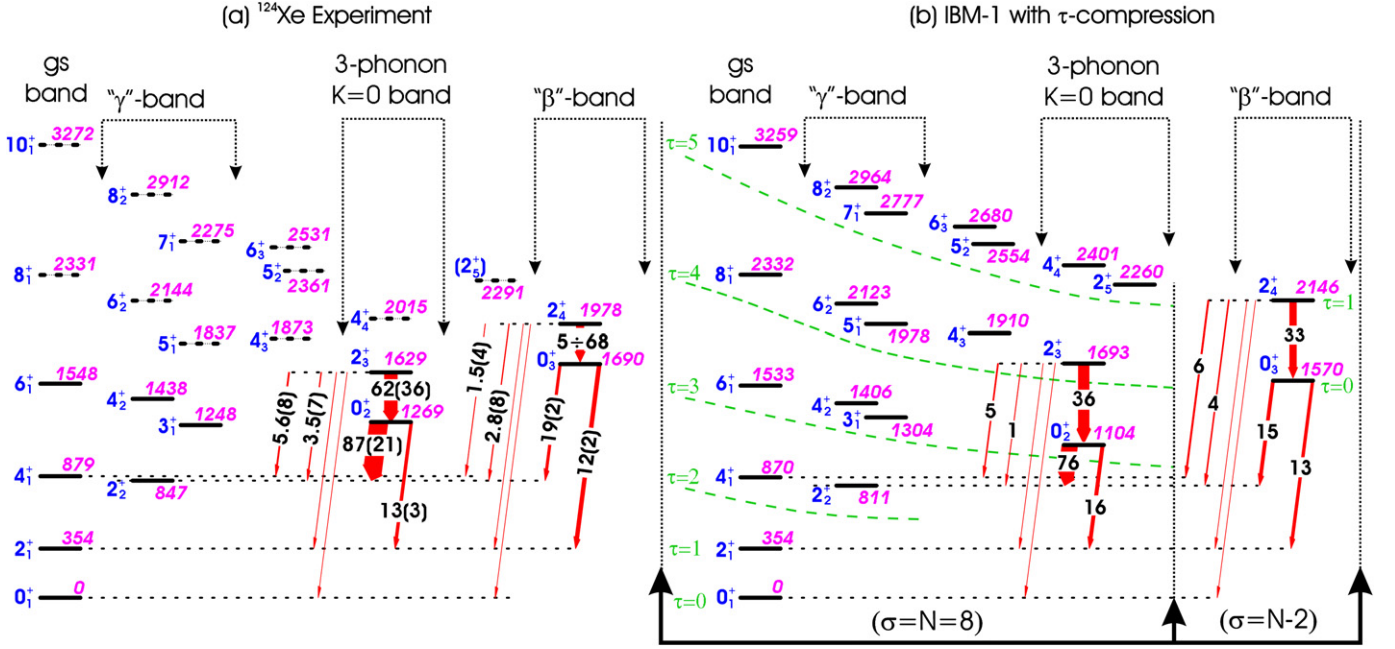


Fig. 2. (Color online.) (a) Low-energy positive-parity levels of  $^{124}\text{Xe}$ . Levels observed in the present experiment are represented by solid lines. (b)  $sd$ -IBM-1 calculation for  $^{124}\text{Xe}$  [16]. The eigenstates are arranged in  $(\tau, \sigma)$  multiplets according to the  $O(6)$  dynamical symmetry, as suggested in Ref. [16]. Since in Ref. [16] the  $\sigma$  quantum numbers are assigned tentatively, they are presented in parentheses. The arrows represent the  $E2$  transitions of off-yrast, quasi- $K=0$  levels of particular interest. The thickness of the arrows and the numbers associated with them (for transitions with  $B(E2) \geq 1$  W.u.) are the absolute  $B(E2)$  values in W.u.

Indeed, the data for transitions between the states tentatively assigned to the  $\sigma = N$  multiplet typically concur to a large extent with the  $O(5)$  ( $\Delta\tau = \pm 1$ ) selection rules (see Table 1): Those  $E2$  transitions that violate the  $O(5)$  selection rules are suppressed by about one order of magnitude to a level of  $\sim 1$  W.u., only. In our experiment we were able to determine the  $E2$  transition strengths for the decays of off-yrast, low-spin states such as the  $2_3^+$  level at 1629 keV. If classified according to  $O(5)$  symmetry, this state is the lowest one from the  $\tau = 4$  multiplet (see Fig. 2). In agreement with the  $O(5)$  selection rules, it decays to the  $0_2^+$  ( $\tau = 3$ ) state by a collective  $E2$  transition. The other transitions observed in the decay of the  $2_3^+$  state are forbidden in the exact  $O(6)$  symmetry and, indeed, their experimental  $E2$  strengths are weak. Moreover, the absolute  $B(E2)$  values for these transitions clearly reflect the degree of  $\tau$ -forbiddenness. The  $2_3^+ \rightarrow 0_1^+$  transition, which corresponds to  $\Delta\tau = 4$ , is about two orders of magnitude weaker than the allowed  $2_3^+ \rightarrow 0_2^+$  decay while, for the  $\Delta\tau = 2$  transitions, this suppression factor is about 10 (see Fig. 2(a)). Altogether, the decay of the  $2_3^+$  state in  $^{124}\text{Xe}$  illustrates the degree of realization of the  $O(5)$  selection rules for  $E2$  transitions between highly excited, off-yrast states rather well. To our knowledge, the  $2_3^+$  state in  $^{124}\text{Xe}$  is the first case of an off-yrast  $\tau = 4$  state in a nucleus of the  $A = 130$  mass region whose absolute  $E2$  decay strengths are measured. In terms of the geometrical collective model [7], the  $0_2^+$  and the  $2_3^+$  states can be considered as the head and the first member of the quasi- $(K=0)$  three-quadrupole phonon band. The absolute  $B(E2)$  value between them is a measure of the collectivity in this excited  $K=0$  band. In the case of  $^{124}\text{Xe}$ , the results indicate (see Table 1) that the collectivity is comparable to that of the ground state band.

The  $B(E2)$  value for the  $4_1^+ \rightarrow 2_2^+$  transition (albeit with a large uncertainty) represents the largest deviation between the  $E2$  data on  $^{124}\text{Xe}$  and the  $O(5)$  selection rules for levels corresponding to  $\sigma = 8$ . However, this transition has not been observed directly (see Table 1), but was inferred instead (with a large uncertainty) from the CE yield of the  $4_1^+$  state, assuming that a direct  $E4$  population from the ground state is not larger than 26 W.u. ( $E4$ ).

With the  $0_3^+$  and  $2_4^+$  states, the data include a level structure that does not fit into the  $\sigma = N = 8$   $O(6)$  family. At first glance, it is tempting to interpret this structure as the bottom of the excited  $O(6)$  family with  $\sigma = N - 2$ , as was done in Ref. [16]. If this interpretation was correct, the  $E2$  decays of these levels to the lower lying structure with  $\sigma = N$  would be forbidden, due to the  $O(6)$  selection rules. However, from the Coulomb excitation yields,  $E2$  transition rates of 11.9(17) W.u. and 18.5(17) W.u. follow for the decays of the  $0_3^+$  state at 1690 keV to the  $2_1^+$  and  $2_2^+$  levels, respectively. These  $E2$  strengths are mildly collective, at least; an observation in severe conflict with the exact  $O(6)$  selection rules. Therefore, we must conclude that, for  $^{124}\text{Xe}$ , the  $O(6)$  symmetry appears to be severely broken rather than somewhat perturbed, as has been assumed before.

The qualitative analysis of the decay rates shows that the new data on the absolute  $E2$  strengths in  $^{124}\text{Xe}$  agree to a large extent with the  $\Delta\tau = \pm 1$  selection rules, but are in severe conflict with the  $\Delta\sigma = 0$  selection rules. This fact leads to the hypothesis that the  $O(5)$  symmetry is predominantly preserved while the  $O(6)$  symmetry is broken in  $^{124}\text{Xe}$ . As a consequence, it is incorrect to use the  $\sigma$  quantum number to label the states, as had been suggested in Ref. [16]. We stress that, at the time of Ref. [16], absolute  $E2$  rates for the  $2_4^+$  and  $0_3^+$  states were not available. A mere branching ratio of two  $E2$  transitions, both forbidden in the exact symmetry, is apparently not a reliable signature for the presence of  $O(6)$  symmetry. For the purpose of the discussion from this point on we will refer to the structures built on the  $0_1^+$ ,  $2_2^+$ ,  $0_2^+$  and  $0_3^+$  states in  $^{124}\text{Xe}$  as the ground state band, the quasi- $\gamma$  band, the quasi- $(K=0)$  three-quadrupole phonon band and the quasi- $\beta$  band, respectively, as indicated on the top of Fig. 2.

At this point of the discussion we are left with the following questions: Do the new experimental data on absolute transition strengths for the decay of the structure based on the  $0_3^+$  state of  $^{124}\text{Xe}$  fit at all into a consistent  $sd$ -IBM-1 description of this nucleus? If so, what is the amount of  $O(6)$  symmetry breaking in  $^{124}\text{Xe}$ ?

**Table 1**  
Measured properties of the levels and  $\gamma$ -ray transitions in  $^{124}\text{Xe}$ . The absolute  $E2$  strengths are compared to  $sd$ -IBM-1 calculations (right-most column, IBM parameters from [16]).

$E_{\text{level}}$ (keV)	$J^\pi$	$E_\gamma$ (keV)	$I_\gamma$	$J_{\text{final}}^\pi$	Transition strength <sup>a</sup>	
					Expt.	IBM-1 <sup>b</sup>
354	$2_1^+$	354	10 <sup>6</sup> (79)	$0_1^+$	57.7(15) <sup>c</sup>	57.7
847	$2_2^+$	493	10019(80)	$2_1^+$	64(5) <sup>d</sup>	61.24
		847	3332(12)	$0_1^+$	1.45(12)	1.47
879	$4_1^+$	525	10297(75)	$2_1^+$	67.6(19) <sup>c</sup>	85.08
		32 <sup>e</sup>		$2_2^+$	92(58)	0.06
1248	$3_1^+$	894 <sup>f</sup>	24(2)	$2_1^+$	2.33(38) <sup>d</sup>	2.20
		401	17(2)	$2_2^+$	95(19) <sup>d</sup>	65.69
		369 <sup>e</sup>	3(1) <sup>g</sup>	$4_1^+$	26(12) <sup>d</sup>	20.71
1269	$0_2^+$	915	130(2)	$2_1^+$	13.2(31)	16.12
		422	18(2)	$2_2^+$	87(21)	76.45
1438	$4_2^+$	591	80(2)	$2_2^+$	66(12)	48.48
		560	39(2)	$4_1^+$	35(6) <sup>d</sup>	33.53
		1084 <sup>f</sup>	1.5(8) <sup>g</sup>	$2_1^+$	0.058(11)	0.33
1548	$6_1^+$	670	54(2)	$4_1^+$	90(18)	96.95
1629	$2_3^+$	1629	154(3)	$0_1^+$	0.315(49)	0.07
		1274	87(4)	$2_1^+$	0.613(68)	0.02
		750	56(2)	$4_1^+$	5.55(79)	4.50
		782	44(2)	$2_2^+$	3.54(71)	1.03
		360 <sup>e</sup>	30(16) <sup>g</sup>	$0_2^+$	62(36)	35.85
1690	$0_3^+$	1336 <sup>f</sup>	81(3)	$2_1^+$	11.9(17)	12.75
		843 <sup>f</sup>	13(2)	$2_2^+$	18.5(17)	14.85
1898	$3_1^-$				0.123(24) <sup>h</sup>	
		1544	1179(9)	$2_1^+$		
		1020	113(3)	$4_1^+$		
1978	$2_4^+$	1051	41(2)	$2_2^+$		
		1131 <sup>f</sup>	23(4)	$2_2^+$	2.75(84)	4.39
		1978 <sup>e</sup>	15(4) <sup>g</sup>	$0_1^+$	0.11(2)	0.10
		1624 <sup>e</sup>	11(3) <sup>g</sup>	$2_1^+$	0.21(7)	0.15
		1100 <sup>f</sup>	11(2)	$4_1^+$	1.47(38)	6.36
2226	$5^{(-)}$	288 <sup>e</sup>		$0_3^+$	5–68	33
		1348 <sup>f</sup>	27(2)	$4_1^+$		
2291	$(2_5^+)$	1444 <sup>f</sup>	35(6)	$2_2^+$		
		1413 <sup>f</sup>	5(1)	$4_1^+$		

<sup>a</sup>  $B(E2)$  values are given in W.u. (1 W.u. =  $36.7e^2 \text{ fm}^4$ ), and the  $B(E3; 0_1^+ \rightarrow 3_1^-)$  value is given in  $e^2 b^3$ .

<sup>b</sup>  $E2$  transition strengths from a numerical IBM-1 calculation with parameters from Ref. [16].

<sup>c</sup> From Ref. [19].

<sup>d</sup> The multipole mixing ratio of this transition is adopted from Ref. [16].

<sup>e</sup> This transition is not observed directly, but it is included in the calculations for the Coulomb excitation cross-sections for a best match with the data.

<sup>f</sup> This transition was observed only in coincidence spectra.

<sup>g</sup> Determined through the branching ratio from Ref. [16] or National Nuclear Data Center (<http://www.nndc.bnl.gov>).

<sup>h</sup> The  $B(E3; 0_1^+ \rightarrow 3_1^-)$  value determined from our data. In Ref. [25] a value of  $B(E3)^\uparrow = 0.091(10)e^2 b^3$  is reported.

We now turn to the results of the numerical  $sd$ -IBM-1 calculation for  $^{124}\text{Xe}$  presented in Ref. [16]. In the present study, the absolute  $E2$  transition strengths were calculated using the same IBM Hamiltonian:

$$H = \epsilon n_d + \left( \lambda + \frac{2}{5} \beta \right) L.L + \kappa Q.X . Q.X + 4\beta T^{(3)} . T^{(3)} \quad (1)$$

and the parameters proposed by Werner et al. in Ref. [16]: with  $\epsilon_W = 0.729 \text{ MeV}$ ,  $\beta_W = -19.65 \text{ keV}$ ,  $\lambda_W = 9.91 \text{ keV}$ ,  $\chi_W = -0.257$ ,  $\kappa_W = -34.91 \text{ keV}$  and  $e_B = 0.14224e^2 b^2$ . For a more de-

tailed discussion on the choice of the parameters we refer the reader to Ref. [16]. The calculations were done using the code PHINT [29]. The results from this numerical IBM calculation are presented in the right-most column in Table 1. Except for the  $2_1^+ \rightarrow 0_1^+$  transition, the calculated absolute  $E2$  transition strengths must be considered as predictions. The agreement between the calculated and the experimental  $B(E2)$  values is strikingly good for all observed  $E2$  transitions, except for the  $4_1^+ \rightarrow 2_2^+$  rate, a point which was addressed above.

In order to document the noteworthy good agreement between the theoretical predictions (outside of any dynamical symmetries) and the data on 25 absolute  $E2$  transition rates, we draw attention to the decays of the excited quasi- $(K=0)$  structures (see Fig. 2). All four  $E2$  decay strengths of the  $0_{2,3}^+$  states have been correctly predicted within a precision of about 25%. Also, the  $E2$  decay rates of the  $2^+$  levels on top of those  $0^+$  quasi-band heads are predicted quite well. The  $2_3^+$  state at 1629 keV decays to the  $0_2^+$  level with a collective  $E2$  transition in agreement with the predictions of the IBM. The  $2_4^+$  state at 1978 keV is observed to decay by weak transitions to the levels below the  $0_3^+$  state, again in agreement with the IBM results. The IBM calculations predict a collective  $2_4^+ \rightarrow 0_3^+$   $E2$  transition with a strength well within the experimentally estimated limits (see Fig. 2). We conclude that the structure built on top of the  $0_3^+$  state of  $^{124}\text{Xe}$  is accounted for well within the framework of the general  $sd$ -IBM-1 in a consistent way, as are the other lower-lying collective excitations. The quantitative agreement between the experimental energies and  $B(E2)$  values and the IBM calculations indicates that quadrupole collectivity persists, even for off-yrast states, to quite high excitation energy.

The present  $sd$ -IBM calculation also make apparent the breaking of the  $O(6)$  symmetry observed in the experimental data. To illustrate this fact, we have projected the wave functions of the first few  $0^+$  and  $2^+$  IBM states to the  $O(6)$  basis  $\{|J^\pi\rangle^{(\sigma,\tau)}\}$ . These results are presented in Fig. 3. It is obvious that neither  $\tau$  nor  $\sigma$  are perfect quantum numbers, of course. However,  $\tau$  quantum numbers are usually quite well preserved which indicates that  $O(5)$  is the relevant symmetry. The components with “correct”  $\tau$  quantum number exhaust about 70% or more of the total wave functions. The small admixtures with different  $\tau$ s are such that the deviations from the  $O(5)$  selection rules can easily be explained. For example, the wave function of the  $0_2^+$  state, the band head of the three phonon  $K=0$  structure (Fig. 2(b)), contains a small component with  $(\sigma=8, \tau=0)$  which has an amplitude of about 3.4% (see Fig. 3(a)). This component makes possible an allowed ( $\Delta\sigma=0, \Delta\tau=-1$ )  $E2$  transition to the main component of the  $2_1^+$  state which has the “correct”  $(\sigma=8, \tau=1)$  quantum numbers and an amplitude of about 61%. In the same time, the main component of the  $0_2^+$  state with  $(\sigma=8, \tau=3)$  quantum numbers can make an allowed transition to the component of the  $2_1^+$  state with  $(\sigma=8, \tau=2)$ . Analogously, the components with  $(\sigma=6, \tau=0)$  and  $(\sigma=4, \tau=0)$  of the  $0_2^+$  state can make allowed transitions to the components with  $(\sigma=6, \tau=1)$  and  $(\sigma=4, \tau=1)$  of the  $2_1^+$  state (see Fig. 3). All these  $\Delta\tau$  allowed contributions may add up and result in the mildly collective  $0_2^+ \rightarrow 2_1^+$  transition which is observed experimentally (see Fig. 2(a)). In the same way the small components with “incorrect”  $\tau$  and  $\sigma$  in the wave functions of the  $0_3^+$  and the  $2_1^+$  IBM states are the main reason for the existence of the otherwise forbidden transition  $0_{\beta,n}^+ \rightarrow 2_1^+$  while main contributions to the collective  $E2$  transition between the  $2_4^+$  and the  $0_3^+$  states come mostly from components with  $\Delta\tau = \pm 1$ .

The  $\sigma$  quantum numbers are, however, totally dispersed (see Fig. 3). Even the ground state contains only 53.5% of  $\sigma = N = 8$ . For the states which were thought to belong to the  $\sigma = N - 2$  representation, the  $0_3^+$  and the  $2_4^+$  levels, the  $\sigma$  quantum number



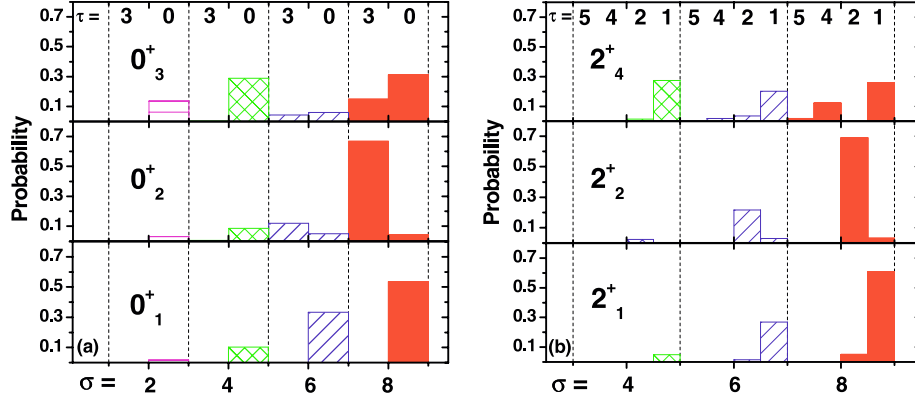


**Fig. 3.** (Color online.) Squared amplitudes of the components with different  $(\sigma, \tau)$  values of the  $0_{1,2,3}^+$  (a) and the  $2_{1,2,4}^+$  (b) *sd*-IBM-1 wave functions.

is completely diluted. In fact, the components with  $\sigma = 6$  account only for 25.9% and 10.2% of the total wave functions of these IBM states (see Fig. 3). While the IBM is very well suited to describe the  $\gamma$ -soft nuclei in the  $A \approx 130$  mass region, the present calculations also confirm our conclusion that the nucleus  $^{124}\text{Xe}$  lies outside the region of O(6) symmetry.

In order to quantify to what extent the dynamical symmetries break down in  $^{124}\text{Xe}$ , we investigated the fluctuations in the quantum number of states, defined as  $\Delta q = \sqrt{\langle q^2 \rangle - \langle q \rangle^2}$ , where  $q$  represents the quantum number related to the symmetry under consideration. An analysis of the quantum-number fluctuations is preferable over the conventional analysis of the wave function amplitudes which has been done above, because it provides one number which is independent of the basis representation. This number enables us to compare the realization of a symmetry in different dynamical systems on a quantitative basis. In a case of exact symmetry,  $\Delta q$  is 0. All the other cases represent a broken-symmetry situation. It is tempting to classify those using  $\Delta q$ . The scale of such classification depends on the minimum step the quantum number  $q$  can change by, denoted  $\delta q_{\min}$ . In order to motivate a reasonable classification scheme, we have assumed that, for broken symmetries, the quantum numbers are normally distributed. Then the case of broken symmetry can be subdivided on two cases depending on how the Full-Width-Half-Maximum (FWHM) of the distribution of quantum numbers  $q$  compares to the  $\delta q_{\min}$ . If  $\text{FWHM} \leq \delta q_{\min}$  we consider the broken symmetry to be *perturbed* only, otherwise ( $\text{FWHM} > \delta q_{\min}$ ) the symmetry is considered *dissolved*. However, in the case of a normal distribution, the quantum-number fluctuation is equal to the standard deviation of the normal distribution. This allows the above definition of perturbed and dissolved symmetry to be refined by introducing a classification value  $\Delta q_{\text{class.}} \equiv \delta q_{\min} / (2\sqrt{2\ln 2})$ . We consider the symmetry to be *perturbed, but dominant*, if the fluctuations in the quantum number is  $\Delta q \leq \Delta q_{\text{class.}}$ , otherwise ( $\Delta q > \Delta q_{\text{class.}}$ ) we consider the symmetry related to this quantum number to be *dissolved*. For example, the quantum number  $\sigma$  changes with a minimum step  $\delta\sigma_{\min} = 2$ . Then, the classification value for the fluctuations in the  $\sigma$  quantum number is  $2/(2\sqrt{2\ln 2})$ . If the fluctuations in the  $\sigma$  quantum number are larger than 0.849, we consider the O(6) symmetry dissolved in the state of interest.

Since the  $\Delta q$  values are related to the detailed structure of the wave functions, they impact the  $E2$  transition rates directly. In order to disentangle the influences of different symmetries, states whose decay is sensitive to a particular selection rule have to be chosen. In the case of  $^{124}\text{Xe}$ , the band heads of the quasi-“ $\beta$ ” structure and the quasi-“ $\gamma$ ” structure are the obvious choices. In terms of the O(6) selection rules, the  $2_{\nu,\gamma}^+ \rightarrow 0_1^+$  tran-

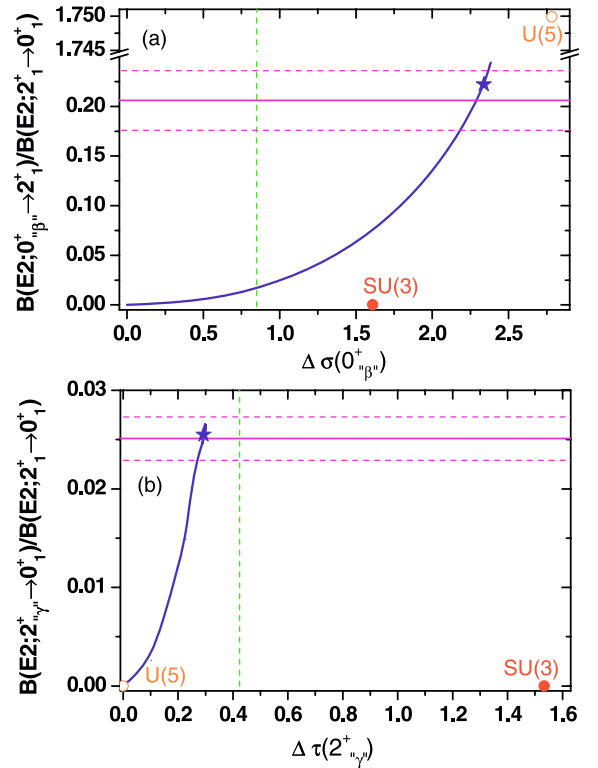


**Fig. 4.** (Color online.) Evolution of the  $B(E2; 2_{\nu,\beta}^+ \rightarrow 2_1^+) / B(E2; 2_1^+ \rightarrow 0_1^+)$  (a) and the  $B(E2; 2_{\nu,\gamma}^+ \rightarrow 0_1^+) / B(E2; 2_1^+ \rightarrow 0_1^+)$  (b) ratios as functions of  $\Delta\sigma$  and  $\Delta\tau$  (solid curves) on the linear trajectory from the exact O(6) symmetry to the point defined by the IBM parameters of Ref. [16] (stars). The vertical dashed lines represent the classification values of  $\Delta\sigma$  and  $\Delta\tau$  beyond which the respective symmetry is dissolved. The circles represent the values of the respective ratios and the fluctuations at U(5) (open circles) and SU(3) (filled circles) dynamical symmetries of IBA. The horizontal lines represent the experimental values in  $^{124}\text{Xe}$ .

sition is  $\sigma$ -allowed and  $\tau$ -forbidden, while the  $0_{\nu,\beta}^+ \rightarrow 2_1^+$  is a  $\sigma$ -forbidden- $\tau$ -allowed transition. We traced the evolution of the  $B(E2; 2_{\nu,\beta}^+ \rightarrow 0_1^+) / B(E2; 2_1^+ \rightarrow 0_1^+)$  and the  $B(E2; 0_{\nu,\beta}^+ \rightarrow 2_1^+) / B(E2; 2_1^+ \rightarrow 0_1^+)$  ratios as functions of  $\Delta\tau$  and  $\Delta\sigma$  on the trajectory through the parameter space of the IBM-1 from the exact O(6) symmetry to the point defined by the model parameters of Ref. [16] (see Fig. 4). This trajectory is defined by the Hamiltonian (1) with the following parametrisation:  $\beta(a) = \beta_{O(6)} + a(\beta_W - \beta_{O(6)})$ ,  $\epsilon(a) = \epsilon_W a$ , and  $\chi(a) = \chi_W a$ . Obviously, when  $a = 1$  the

above parametrisations represents exactly the original Hamiltonian  $H_W$  used in Ref. [16], while, in the case of  $a = 0$ , Eq. (1) represents an IBM Hamiltonian in the exact  $O(6)$  symmetry. The parameter  $\beta_{O(6)} = -0.455$  keV, was chosen to produce the head of the  $\sigma = N - 2$  structure as the third  $0^+$  state in the exact  $O(6)$  symmetry ( $a = 0$ ). From this point on, this  $0^+$  state was traced on the basis of its unique feeding and decay pattern to the  $0_3^+$  which results from the  $sd$ -IBM-1 calculation for  $^{124}\text{Xe}$  ( $a = 1$ ). No crossings with other  $0^+$  states were observed on the way. A comparison between the resulting evolution of the  $B(E2; 0_{\alpha\beta}^+ \rightarrow 2_1^+)/B(E2; 2_1^+ \rightarrow 0_1^+)$  ratio and the experimental value in  $^{124}\text{Xe}$  (Fig. 4(a)) provides  $\Delta\sigma_{\text{exp}}(0_3^+; ^{124}\text{Xe}) = 2.29_{-0.11}^{+0.07}$ , a value well beyond the classification value of 0.849. In Fig. 4(a) the fluctuations in the  $\sigma$  quantum number for the other dynamical symmetries,  $U(5)$  and  $SU(3)$ , are also presented. Both of them are above the classification value which demonstrate the usefulness of such a criteria for quantifying the degree of  $O(6)$  symmetry breaking. The obtained value of  $\Delta\sigma_{\text{exp}}$  for the  $0_{\alpha\beta}^+$  state of  $^{124}\text{Xe}$  not only confirms our previous conclusion that the  $O(6)$  symmetry is broken, but also indicates that the degree of breaking is comparable to the one in the other dynamical symmetries, i.e. in  $^{124}\text{Xe}$  the  $O(6)$  symmetry is actually completely dissolved. An analogous analysis for the  $B(E2; 2_{\alpha\gamma}^+ \rightarrow 0_1^+)/B(E2; 2_1^+ \rightarrow 0_1^+)$  ratio tells a different story for the  $O(5)$  symmetry (Fig. 4(b)); even though the experimental ratio is close to the ratio corresponding to the maximum possible fluctuations in the  $\tau$  quantum number on the trajectory we have investigated (afterwards it bends back down), it is still well below the classification value  $\Delta\tau_{\text{class.}} = 1/(2\sqrt{2\ln 2})$ . The experimental value of  $\Delta\tau_{\text{exp}}(2_2^+; ^{124}\text{Xe}) = 0.292(22)$  indicates that the  $O(5)$  symmetry is only slightly perturbed. Indeed, this value is closer to 0, where the value for fluctuations in the  $\tau$  quantum numbers for the  $U(5)$  symmetry abides ( $U(5)$  includes  $O(5)$  symmetry, i.e., no fluctuations in the  $\tau$  quantum number are present in  $U(5)$  symmetry) than to the value for the fluctuations expected at the  $SU(3)$  symmetry, which is well beyond the classification value of 0.425 (see Fig. 4(b)). We stress that such an analysis is made possible only by the comprehensive set of absolute values of  $E2$  transition rates available from the present projectile Coulomb excitation measurements on a light target.

In summary, we have studied  $^{124}\text{Xe}$  using projectile Coulomb excitation. The data yield 25 absolute  $E2$  transition strengths between low spin states. The experimentally observed level energies, branching ratios and the absolute transition strengths are reproduced well by an  $sd$ -IBM-1 calculation [16] outside of the  $O(6)$  dynamical symmetry. The new data allow the symmetry breaking to be investigated by relating the fluctuations in the quantum numbers directly to the experimental observables. Using this approach, we have quantitatively shown that, in  $^{124}\text{Xe}$ , the  $O(6)$  symmetry is completely dissolved while the  $O(5)$  symmetry is only slightly perturbed. It is therefore important the issue be investigated further which requires more  $E2$  transition rates for high-lying off-yrast

states of nuclei that are currently being viewed as close to the  $O(6)$  symmetry be measured and analysed with the method we have proposed here. Clearly  $^{196}\text{Pt}$  becomes a very interesting case.

## Acknowledgements

We thank F. Iachello, A. Leviatan, P. Van Isacker, P. von Brentano and R.F. Casten for fruitful discussions. V.W. and G.R. thank the Helmholtz International Center for FAIR within the LOEWE program for support. This work is supported by the US NSF within contract PHY-0245018, by the US Department of Energy, Office of Nuclear Physics, under contracts DE-AC02-06CH11357, DE-FG02-04ER41334 and DE-FG02-91ER40609, by the Bulgarian NSF within contract DO 02-219, by the German-Bulgarian exchange program under grants D/08/02055 and D002-25, and by the DFG under grants JO391/3-2, SFB 634 and Pi393/2-1.

## References

- [1] A. Arima, F. Iachello, Phys. Rev. Lett. 35 (1975) 1069.
- [2] F. Iachello, A. Arima, The Interacting Boson Model, Cambridge University Press, Cambridge, 1987.
- [3] A. Arima, F. Iachello, Ann. Phys. (N.Y.) 99 (1976) 253.
- [4] A. Arima, F. Iachello, Ann. Phys. (N.Y.) 111 (1976) 201.
- [5] A. Arima, F. Iachello, Phys. Rev. Lett. 40 (1978) 385.
- [6] A. Bohr, Mat. Fys. Medd. K. Dan. Vidensk. Selsk. 26 (1952), No. 14.
- [7] L. Wilets, M. Jean, Phys. Rev. 102 (1956) 786.
- [8] R.F. Casten, D.D. Warner, Rev. Mod. Phys. 60 (1988) 389, and the references therein.
- [9] R.F. Casten, P. von Brentano, Phys. Lett. 152 (1985) 22.
- [10] D.D. Warner, R.F. Casten, Phys. Rev. Lett. 48 (1982) 1385; D.D. Warner, R.F. Casten, Phys. Rev. C 28 (1983) 1798.
- [11] P. Van Isacker, Nucl. Phys. A 465 (1987) 497.
- [12] J.A. Cizewski, et al., Phys. Rev. Lett. 40 (1978) 168.
- [13] H.G. Borner, J. Jolie, S. Robinson, R.F. Casten, J.A. Cizewski, Phys. Rev. C 42 (1990) R2271.
- [14] U. Neuneyer, et al., Nucl. Phys. A 607 (1996) 299.
- [15] A. Gade, et al., Nucl. Phys. A 665 (2000) 268.
- [16] V. Werner, H. Meise, I. Wiedenhover, A. Gade, P. von Brentano, Nucl. Phys. A 692 (2001) 451.
- [17] X.W. Pan, T. Otsuka, J.Q. Chen, A. Arima, Phys. Lett. B 287 (1992) 1.
- [18] J. Srebny, et al., Nucl. Phys. A 557 (1993) 663c.
- [19] B. Saha, et al., Phys. Rev. C 70 (2004) 034213.
- [20] A. Leviatan, A. Novoselsky, I. Talmi, Phys. Lett. B 172 (1986) 144.
- [21] P. Von Brentano, A. Gelberg, S. Harissopolos, R.F. Casten, Phys. Rev. C 38 (1988) 2386.
- [22] I.Y. Lee, Nucl. Phys. A 520 (1990) 641c.
- [23] W.P. Alford, R.E. Anderson, P.A. Batay-Csorba, R.A. Emigh, D.A. Lind, P.A. Smith, C.D. Zafiratos, Nucl. Phys. A 323 (1979) 339.
- [24] W.B. Walters, J. Rikovska, N.J. Stone, T.L. Shaw, P. Walker, I.S. Grant, Hyper. Inter. 43 (1988) 343.
- [25] W.F. Mueller, et al., Phys. Rev. C 73 (2006) 014316.
- [26] K. Alder, A. Winther, Coulomb Excitation, Academic Press, New York, 1966.
- [27] H. Ower, J. Gerl, H. Scheit, computer program CLX.
- [28] G. Rainovski, N. Pietralla, T. Ahn, L. Coquard, C.J. Lister, R.V.F. Janssens, M.P. Carpenter, S. Zhu, J. Jolie, AIP Conf. Proc. 1090 (2009) 263.
- [29] O. Scholten, Computer codes PHINT and FBEM, KVI internal report No. 63, 1979.